







DAILY HEAT STRESS IN KRAKÓW IN THE WARM PERIOD 2012–2022 BASED ON HOURLY METEOROLOGICAL MEASUREMENTS AND RADIATIVE FLUXES DERIVED FROM SATELLITE SYSTEMS

JOANNA WIECZOREK^{1*} , BOGDAN BOCHENEK¹ , TOMASZ STRZYŻEWSKI¹,
MONIKA J. HAJTO^{2,3} , PIOTR SEKUŁA¹ , ANITA BOKWA³ , MIROSŁAW ZIMNOCH⁴ 

Abstract. This paper aims to present an assessment of the hourly structure of the thermal environment in the warm period of the year. Special attention was paid to the conditions potentially resulting in heat stress for citizens of Kraków's central district. Two approaches were used to analyse the hourly data: 1) a criterion of thermal threshold $>30^{\circ}\text{C}$, as potentially generating heat stress, which is included in meteorological warnings issued in Poland, and 2) a criterion based on physiological responses described by the value of the Universal Thermal Climate Index (UTCI) $>32^{\circ}\text{C}$, which corresponds to conditions of strong heat stress for the human thermoregulatory system. The data of basic meteorological characteristics of one-hour timespan resolution from measurements in AGH station located at Reymonta Street in Kraków covering the period 2012–2022 were adopted in the study. Shortwave direct and diffuse and longwave radiation fluxes corresponding to the station's location grid were derived from the Eumetsat LSA SAF MSG satellite remote-sensing system and used for Mean Radiant Temperature (Tmrt) and UTCI hourly calculations. Thermal environment conditions expressed by $T_{\text{air}} \geq 30^{\circ}\text{C}$, which could lead to heat stress, occurred in less than 2% of hourly terms (931 from 47,044) in the months April–September in the 11-year period. Far more terms were assessed as “with adverse conditions leading to heat stress”: 2,215 cases when $\text{UTCI} \geq 32^{\circ}\text{C}$. In view of the above, it is worth highlighting that more than half of the negative and oppressive weather conditions resulting in heat stress may be neglected in risk assessments and predictions using only the basic thermal criterion.

Key words: prolonged exposure to heat, mean radiant temperature, human heat load, urban climate, UTCI

Introduction

Changes in the thermal environment pose one of the biggest challenges of climate adaptation for citizens of urbanised regions. Almost all Polish cities that joined the MPA44 project (Urban Adaptation Plans for Climate Change), including Kraków, have identified the public health sector

as the most vulnerable to progressing climate change (*Ministry of the Environment... 2023*). As the European Commission Project PESETA IV highlights, each year more than 100 million Europeans (in southern Europe mainly) will be exposed to an intense heatwave, compared to nearly 10 million annually nowadays. And with the 2°C scenario, which unfortunately seems feasible, this grows to nearly 170 million per year in 2100,

¹ Institute of Meteorology and Water Management – National Research Institute, Centre of Numerical Weather Prediction; Podleśna 61, 01-673 Warsaw; e-mail: joanna.wieczorek@imgw.pl, ORCID: 0000-0001-6472-257X; e-mail: bogdan.bochenek@imgw.pl, ORCID: 0000-0002-7096-7589; e-mail: tomasz.strzyzewski@imgw.pl; e-mail: piotr.sekula@imgw.pl, ORCID: 0000-0001-7092-5402

² Institute of Meteorology and Water Management – National Research Institute, National Meteorological Protection Centre, Satellite Remote Sensing Department; Piotra Borowego St. 14, 30-215 Cracow; e-mail: monika.hajto@imgw.pl, ORCID: 0000-0003-2094-4140

³ Jagiellonian University, Faculty of Geography and Geology, Institute of Geography and Spatial Management; Gronostajowa 7, 30-387 Cracow; e-mail: anita.bokwa@uj.edu.pl, ORCID: 0000-0002-3809-7843

⁴ AGH University of Krakow, Faculty of Physics and Applied Computer Science; Reymont St. 19, 30-059 Cracow; e-mail: zimnoch@agh.edu.pl, ORCID: 0000-0002-0594-9376

*corresponding author

which could be associated with mortality rates as high as 50,000 per year, compared to 2,700 nowadays (EC, Peseta IV Project). In the Central European area, such intense phenomena are likely to occur less frequently, every 3–5 years, but this does not change the need for population adaptation. (Kruger *et al.* 2017). Europeans, most notably those living in northern regions, are not physiologically equipped to deal with excessive heat stress. In addition to the population, so too the infrastructure is not prepared; many cities, such as Paris, were designed as “cool zone cities”. Therefore, there is an urgent need to introduce changes in the urban space that will improve the population’s protection. Paris, for example, is preparing for a 50°C scenario (*Ville de Paris...* 2023). An oppressive thermal environment that forces the implementation of mitigation strategies (e.g., additional cooling) occurs mainly (but not only) during heat waves. If the problem of adaptation is considered from a broader perspective – taking into account the days when the disparity between the level of thermal comfort and thermal conditions is significant (as described by the cooling degree day index [CCD]) – it turns out that the region of Central and Northern Europe will experience the greatest relative change, if the global climate scenario of a 2°C increase comes true instead of 1.5°C (Miranda *et al.* 2023). As stated by Błażejczyk and Twardosz (2023), who analysed the longest available data series for Kraków (1826–2021), average annual Universal Thermal Climate Index (UTCI) values increased at the rate of 0.27°C/10 years. This is in agreement with a general regional trend (Hynčica *et al.* 2023), while the mentioned growth is differentiated for other Polish locations, as reported by Kuchcik *et al.* (2021). On the days when the threshold of UTCI>32°C is exceeded, there is an increase in the mortality of residents in Polish cities (Kuchcik 2021). A clear relationship was documented for June 2019 conditions. The number of deaths attributed to strong heat stress was five times higher than the average for the reference period of 2010–2018. Thermal stress measures were significantly higher – averaged noon UTCI value was larger by 6.8°C and the number of strong heat stress (UTCI 32.1–38.0°C) and very strong heat stress (38.1–46.0°C) days was 5.6 days higher than in the reference period (Błażejczyk *et al.* 2022).

Studies on the evaluation of the extreme heat load cases, comprehensively shown by the UTCI index and its variations in the Polish population, have been carried out by many authors. A detailed

overview can be found in the work of Tomczyk and Matzarakis (2023). In some works, periods of the warmest months relative to multi-year norms were analysed in detail, which was exhaustively referred to in the paper of Twardosz (2023). However, the daily variability of unfavorable conditions potentially resulting in overheating of the body is still insufficiently recognized, as most studies are based on data for selected hours only. A review of studies for cities in Poland is available in the work of Okoniewska (2021). An unfavorable thermal load may occur not only around noon (Pecelj *et al.* 2020). Moreover, the timing of exposure to thermal stress may be crucial from a physiological point of view (Kruger *et al.* 2017). Considering only the criterion of extremes, no such information is taken into account, which may also limit the prominence of the impact of meteorological conditions, if only in media coverage, as pointed out by Sadeghi *et al.* (2021). In addition, the evaluation of “sweltering” days (Kossowska-Cezak 2014) may not be fine enough, especially since the number of hours with a significant heat load can vary. Better recognition of the anatomy of heat and its potential physiological effects should aim to improve assessments and increase awareness of meteorological risks (Di Napoli *et al.* 2018, 2021; Urban *et al.* 2023).

While biometeorological studies assess the thermal environment using various indicators (Błażejczyk *et al.* 2012), most assessments issued as warnings to the public are still based on thermal threshold criteria, excluding the complex impact of other meteorological elements. Only a few meteorological services (from ProClias materials, unpublished) use criteria based on values of biometeorological indicators such as Perceived Temperature (Germany), UTCI (Italy, Croatia), Heat Index (USA, Switzerland) or WBGT (Australia). From the perspective of climate change and thermal challenges for the population, the implementation of detailed assessments is worth the effort. Such assessments can support, for example, impact warnings and recommendations and replace the usual patterns and the use of simple indicators. This is also supported by demographic challenges as populations are ageing. According to Meade *et al.* (2023): “older adults sustain greater increases in heat storage and core temperature during daylong exposure to hot, dry conditions compared with their younger counterparts”.

Conditions that severely stress the human body (classified as UTCI value $\geq 32^\circ\text{C}$) can occur even before the air temperature reaches 30°C. The level of physiological response and possible

health effects at the level of $UTCI > 32^{\circ}\text{C}$ are described in detail by Jendrytzky *et al.* (2012), and applications of UTCI as a prognostic tool in medicine were reviewed in detail by Romaszko *et al.* (2022). The impact of the last severe heat wave, which occurred in June 2019, concerning the Polish population – from an epidemiological point of view was pointed out by Błażejczyk *et al.* (2022).

The purpose of this study is to assess the exposure of residents of downtown Kraków to the occurrence of severe heat stress conditions in the daily course in the months from April to September. The objective UTCI will be used as an assessment tool. Analysis of hourly data from 2012–2022 will help answer the following research questions:

1. When and how often does the strong heat load occur in April to September in Kraków in the daily course?
2. To what extent are the conditions of strong heat load limited to the hours around noon only?
3. Can the number of hours with a strong heat load vary significantly on days defined as “sweltering”?

An important question that this paper will answer is: how many potentially dangerous situations with abundant heat load are omitted if we consider only the evaluation of the thermal environment based on the criterion of 30°C instead of UTCI value 32°C that is described as a realistic physiological risk threshold (Kuchcik 2021). This is, of course, a gross oversimplification; it is impossible to directly compare the physiological effect of a situation with $T_{air} \geq 30^{\circ}\text{C}$ and $UTCI \geq 32^{\circ}\text{C}$. Such a juxtaposition is only meant to indicate the need to move away from thermal perception assessments to more comprehensive assessments of heat stress load, especially in the field of warnings and recommendations.

Study area

Kraków is located in southern Poland, on the Vistula River. The city is located in a river valley going east–west, i.e. in a concave landform. The historical city centre is located at the river valley bottom (at ~ 200 m a.s.l.) and on a tectonic limestone horst (the Wawel Hill), which emerges from the river valley. The northern part of the city belongs to the Kraków-Czestochowa Upland. The southern parts of the city belong partially to the Carpathian Foothills. The Vistula River valley is narrow in the western part of the city, with

a width of about 1 km, and widens to about 10 km in the eastern part. In the western part of the valley, there are several limestone horsts reaching about 350 m a.s.l. Therefore, the city area is surrounded by convex landforms from the south, west and north. Height differences between the valley floor and the hilltops next to the city borders are about 100 m, and the built-up areas do not reach those hilltops. On the valley floor, the land use is most differentiated, while in the convex landforms south and north of the valley, only selected land-use forms can be found. Buildings with more than four floors (districts with blocks of flats) are located mainly in the suburbs. Densely built-up areas are found mainly in the Old Town. The meteorological data used in the present study comes from the meteorological station of AGH University of Kraków, located on the valley floor, in the western part of the valley, and in the city centre in a densely built-up area (Fig. 1).

There are numerous studies on the climate and bioclimate of Kraków (e.g., Niedźwiedz *et al.* 1996; Bokwa 2019), and the following findings are relevant for the present analysis. The location of the city in a concave landform generates various processes in the scale of the local climate which in turn significantly modify the spatial pattern of the meteorological elements, including air temperature. The urban heat island is an element of a complicated spatial pattern of air temperature only and it has to be determined following the method of RMUHI (Relief-Modified Urban Heat Island; Bokwa *et al.* 2015). Heat load in Kraków is very diversified spatially, too. Bokwa and Limanówka (2014) analysed air temperature measurements of 5-minute resolution from 21 points in Kraków and its vicinities and showed that significant differences occur in the number of tropical nights ($t_{min} > 20^{\circ}\text{C}$), very hot days ($t_{max} > 30^{\circ}\text{C}$) and number of heat waves, between urban areas in the valley and rural areas, both in the valley and on the slopes. In the valley bottom with the urban built-up area, the numbers of tropical nights and very hot days are 50% greater than in areas with the same land use but located 50 m higher. During the heat waves, on the valley floor, the air temperature exceeds 30°C for about 30% of the heat wave duration. During the nighttime, air temperature in urban areas is controlled by different factors than during the daytime. In Kraków, the nocturnal air temperature pattern is further complicated by katabatic flows, the formation of cold air reservoirs, and air temperature inversions linked to the mentioned relief impact. Heat stress conditions in Kraków are



Fig. 1. Location of AGH station within Krakow administrative boundary (A), and meteorological and net radiometer sensors on the building (B)

more diversified spatially during the nighttime than during the daytime. Bokwa *et al.* (2019) analysed heat load in Central European cities, including Kraków, during a heat wave. The study confirmed that during the daytime, higher heat load occurs in the valleys' floors than in areas located above, both in rural and urban areas. Błażejczyk and Twardosz (2023) analysed the time series for Kraków from the period 1826–2021 using UTCI and showed a significant increase in the number of days with heat stress ($UTCI > 32^{\circ}\text{C}$) which reached 0.5 days/10 years, but for the period 1941–2021 the rate was much higher, at 2.6 days/10 years. Bokwa *et al.* (2018) showed the current and predicted spatial pattern of heat load for the same cities; the heat load in urban areas of Central Europe, expressed in the mean annual number of summer days, is expected to increase by 2100, comparing to 1971–2000, by 20–50 days, depending on the scenario used (i.e., RCP8.5, RCP4.5 or RCP2.6). The results highlighted above show the need for further studies of the heat load in Kraków, with a special focus on its spatial and temporal variability. In particular, the varied relief in Kraków will be a factor that significantly modifies the variability of thermal stress.

Materials

The basic material consisted of data obtained from the AGH meteorological station located at Reymonta Street in Kraków ($50^{\circ}04'\text{N}$, $19^{\circ}55'\text{E}$,

220 m a.s.l., Fig. 1), in the built-up area of the downtown zone. Data from hourly readings of air temperature, relative humidity and wind speed measured by Vaisala WXT520 compact weather station were used in the analysis. The station is installed on top of a small mast 5 m above the building's flat roof, which is covered with roofing felt, 25 m a.g.l., ~ 2 m from the edge of an upwind building side to minimise the heating effect from the roof.

If at least one of the hourly air temperature values exceeded 30°C , the day was considered a "sweltering day". The completeness of the data set for the April–September period from 2012 to 2022 for the air temperature component was 97.4%. At the AGH station, total long-wave and short-wave radiation fluxes are measured by a Hukseflux NR01 net radiometer, i.e., there are no radiation fractions (direct and diffuse) available, which makes it impossible to estimate the Mean Radiant Temperature (T_{mrt}) according to the VDI methodology (Kántor, Unger 2011). In addition, the set for radiation elements for a given period was incomplete, so it was decided to use alternative sources of measurement data. Since the radiation measurement sensor installed at the AGH station is located on the roof of the building and there are no taller objects in the surrounding area, it was decided to use satellite radiation flux measurement data available for the coordinate area of the station location. Satellite data on radiation fluxes are derived from the measurements taken by the SEVIRI instrument onboard the Meteosat Second Generation (MSG) geostationary satellite. The MSG/

SEVIRI measurement is instantaneously performed every 15 minutes and its spatial resolution is 3 km at a subsatellite point on the equator.

The following EUMETSAT LSA SAF Satellite Application Facility on Land Surface Analysis (LSA SAF) satellite products with spatial resolution of $0.05^\circ \times 0.05^\circ$ (data access at Landsaf 2023) were used:

- MSG Downward Surface Shortwave Radiation Flux Total and Diffuse (MDSSFTD), available every 15 minutes (Carrer *et al.* 2019);
- MSG Daily Albedo (MDAL), available every day (Geiger *et al.* 2008);
- MSG Downward Surface Longwave Flux (MDSLF), available every 30 minutes (Trigo *et al.* 2010);
- MSG Emissivity (MEM), available every day (Peres, DaCamara 2005; Trigo *et al.* 2008);
- MSG Land Surface Temperature (LST) All-Sky (MLST-AS), available every 30 minutes (Martins *et al.* 2019) – the data were used only for the period 1 January 2022–31 December 2022.

Additionally, the GLASS Land Surface Temperature All-Sky (GLST-AS), available every hour with a spatial resolution of $0.05^\circ \times 0.05^\circ$ (Liang *et al.* 2020) from 1 January 2012 to 31 December 2021, was used. MDSSFTD data provides the values of total downward surface shortwave radiation flux (DSSF) together with a fraction of diffuse DSSF. Direct DSSF may then be calculated as the difference between total and diffuse DSSF (Carrer *et al.* 2019). MDAL data enables estimation of reflected DSSF (MDSSFTD multiplied by MDAL). The difference between total and reflected DSSF gives the values of surface net solar radiation. MDSLF data provides the values of downward surface longwave radiation flux (DLSF). MEM and LST (MLST-AS and GLST-AS) data enable estimation of upward surface longwave radiation flux (ULSF) according to the equation: $ULSF = MEM \cdot \sigma \cdot LST^4$, where symbol σ is Stefan-Boltzmann constant $5.67 \cdot 10^{-8} \cdot [W \cdot m^{-2} \cdot K^{-4}]$. Then, surface net thermal radiation may be estimated as the difference between DLSF and USLF. Both datasets – from meteorological measurements at AGH station and MSG satellite were expressed in universal time (UTC).

Methods

The Universal Thermal Climate Index (UTCI) was calculated following the original formula given

by Bröde *et al.* (2012). It takes as inputs the ambient temperature, wind speed, vapour pressure and T_{mrt} . The mean radiant temperature T_{mrt} was calculated according to the approach of Di Napoli *et al.* (2020), using the sixth-order polynomial regression approximation given by Bröde *et al.* (2011). The calculations were approximated using hourly (each hh:00 step) values of total downward surface solar radiation (direct [fdir] and diffuse [fdiff] separately), surface net solar radiation, downward surface thermal radiation, surface net thermal radiation, downward direct surface solar radiation at the surface obtained from the satellite measurements and estimated cosine of the solar zenith angle (CZA) and the radiation intensity of the Sun on a surface perpendicular to the incident radiation direction (dsrp). Both variables were estimated using equations given by Brimi-combe *et al.* (2022). In the hourly terms, when the Sun was below the horizon, a “zero” CZA was put in the main equation and *dsrp* values were calculated as $fdir/CZA$ if $CZA > 0.01$. This approach is not ideal and, depending on the specific atmospheric conditions, may be subject to uncertainty in estimating the incident flux on the perpendicular surface, especially at lower sun positions during sunrise and sunset, which was mentioned by Hogan and Hirahara (2016). In some parts, this is still an unsolved problem, and T_{mrt} is the most challenging to calculate (Kruger *et al.* 2014) or even measure directly using global thermometers (Lindner-Cendrowska, Baranowski 2023).

Two approaches were used to analyse the hourly data in the context of potentially unfavorable heat stress occurrence: 1) criterion of thermal threshold $\geq 30^\circ C$, as it is used to define very hot days in Poland and is applied in preliminary meteorological warnings issued in Poland, and 2) a criterion based on physiological responses described by the value of the UTCI $\geq 32^\circ C$, which corresponds to conditions of strong heat stress for the human thermoregulatory system. The analysis covered a total of 48,312 hourly terms (aggregated in 2,013 days) from April to September in 2012–2022. The data come from the meteorological station of AGH in Kraków ($50^\circ 04' N$, $19^\circ 55' E$). In this set, the number of 1-hour terms with available values of air temperature (T_{air}) and calculated UTCI values was 47,044 and 44,366 records, respectively. Due to the lack of air temperature or radiative fluxes measurements needed to calculate UTCI, 54 days were excluded from the analysis.

The authors postulate that referring to the overarching goal of the work, which is to indi-

cate the physiological burden of heat and its temporal variability, the results should be treated as an approximation of the conditions that the organisms of urban space residents in Kraków must face, due to the mosaic of environmental conditions and the use of urban space at varying levels.

Results

The share of hourly data with air temperature $\geq 30^{\circ}\text{C}$ does not exceed 2% (931 1-hour periods, which were noted in 171 days). A total of 2,215 hourly terms in 448 days with strong heat stress ($\text{UTCI} \geq 32^{\circ}\text{C}$) were experienced in Kraków from 2012 to 2022. The mentioned disparity and the number of terms in the following years are

summarised in Figure 3. In 1,435 cases when $\text{UTCI} \geq 32^{\circ}\text{C}$, the air temperature did not exceed the 30°C threshold. For the cases when the air temperature at the station was $\geq 30^{\circ}\text{C}$, UTCI values were assessed as moderate heat stress (MH) in 131 cases, strong heat stress (SH) in 652 cases, or very strong heat stress (VSH) in 128 cases. Cases with heat stress account for about 20% between April and September (Fig. 2), while by far the largest number occurs between June and August – from moderate (MH) to very strong (VSH) heat stress. The first appearance of strong heat stress (SH) may be noted in April, but so far, it has occurred only in April 2012 (3 times). Cold stress is still more common in this month than heat stress.



Fig. 2. Monthly distribution of UTCI categories based on hourly intervals in Kraków 2012–2022
 SC – strong cold stress ($-27 \leq \text{SH} < -13$), MC – moderate cold ($-13 \leq \text{SH} < 0$), SLC – slight cold ($0 \leq \text{SH} < 9$),
 C – no stress ($9 \leq \text{SH} < 26$), MH – moderate heat stress ($26 \leq \text{SH} < 32$), SH – strong heat stress ($32 \leq \text{SH} < 38$),
 VSH – very strong heat stress ($38 \leq \text{SH} < 46$)

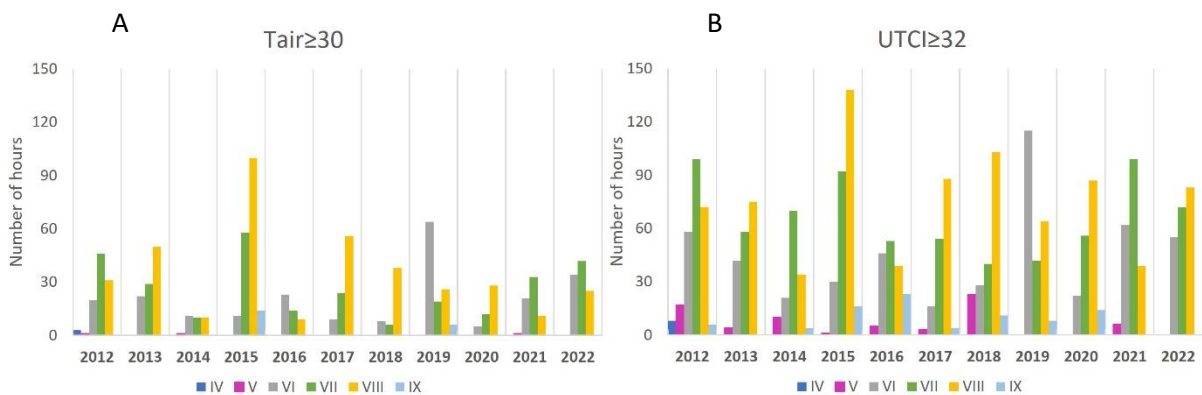


Fig. 3. Annual numbers of hourly values of air temperature $\geq 30^{\circ}\text{C}$ (A) and $\text{UTCI} \geq 32$ (B)

The number of hourly data with the occurrence of abundant heat load is subject to variability determined by the synoptic situation and varied in Kraków in successive seasons (Fig. 3). The highest number of cases with heat load occurred in 2015, at 277, and the lowest number in 2014, at 139. Usually, the highest number of hours with $UTCI \geq 32^\circ C$ occurs in August, but there were years when it occurred in June (2019) or July (2012, 2014, 2021). The pattern is similar for $T_{air} \geq 30^\circ C$, but these conditions are usually limited to June–August. The heat load usually occurs in a wider range of months in a given year or in different proportions (such as in 2022).

During the warm half of the year (April–September), thermal conditions of $T_{air} \geq 30^\circ C$ occurred in Kraków in the range of 8 am to 7 pm UTC, with the highest number of 144 at 14 UTC (4 pm official time). In the case of UTCI, the daily course is similar, but the values $\geq 32^\circ C$ occur from 6 am to 5 pm UTC. The largest number of terms meeting conditions of $UTCI \geq 32^\circ C$ were counted for 12 UTC (308 cases). For each day with the occurrence of at least one $UTCI \geq 32^\circ C$ term, the time of occurrence of the “highest hourly UTCI on a single day” ($UTCI_{high.}$) was checked. The highest hourly values were recorded most often at 13 UTC.

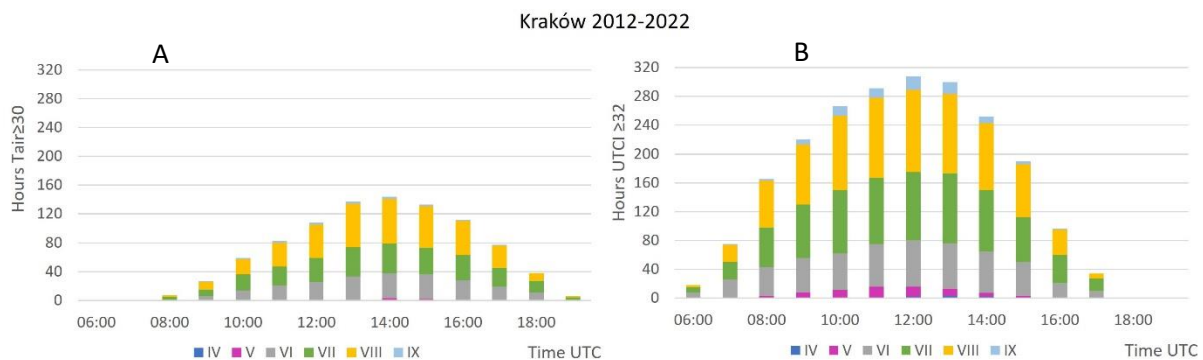


Fig. 4. Number of hours in the daytime with $T_{air} \geq 30^\circ C$ (A) and $UTCI \geq 32^\circ C$ (B)

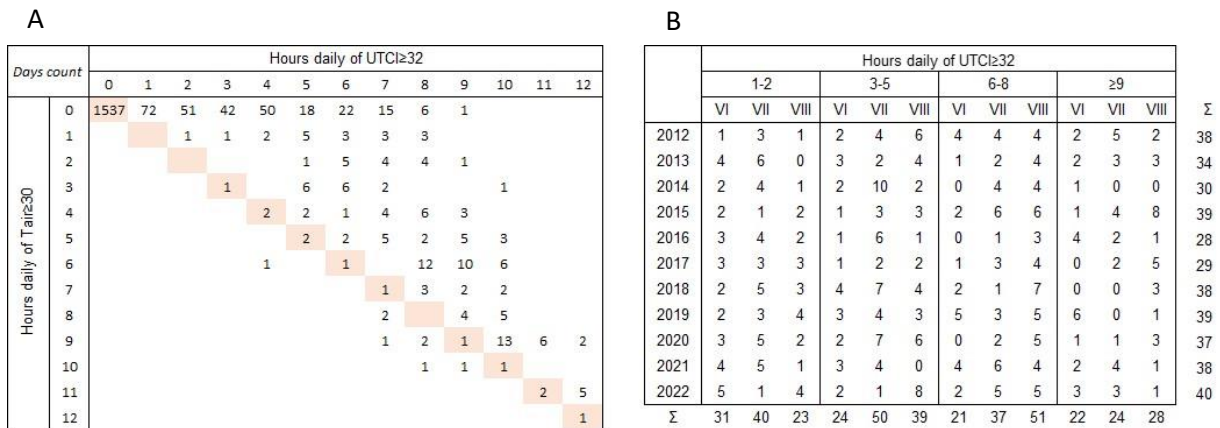


Fig. 5. A – Number of days with $T_{air}/UTCI$ hour intervals 0–12 (heat stress duration), exemplified by the unfavourable conditions
 B – Number of days in successive June–August periods of 2012–2022 of daily count of $UTCI \geq 32^\circ C$ in ranges 1–2, 3–5, 6–8 and above 9 time intervals

In contrast, the highest UTCI value in the analysed set (42.4 on 8 August 2013) occurred at 14 UTC. To answer the question of whether the noon date (UTC_{12}) can be used to approximate the greatest load on the body, the value from 12 UTC was compared with the $UTCI_{high.}$, which came from each day. Claiming that in 99 out of 308 cases

of $UTCI \geq 32^\circ C$ terms, these values were equal. On the remaining 136 days the $UTCI_{high.}$ exceeded the $32^\circ C$ threshold, while $UTCI_{12}$ was still below. In 277 days of all 448 cases, conditions of at least strong heat stress were noted when the hourly T_{air} value was below the $30^\circ C$ threshold.

Usually, severe heat stress occurs over a longer period (if one accepts the generalisation that heat load conditions between the following measurement terms do not change) on days when at the midtown AGH $T_{air} \geq 30^\circ\text{C}$. On days described as “sweltering” ($T_{air} \geq 30^\circ\text{C}$) the disproportion in heat stress duration may be sizable (Fig. 4). The highest number of days with extended exposure to severe stress conditions >6 terms occurs in August, while the incidence of more than nine terms with SH was similar in June, July and August. The most severe conditions of heat stress duration – 12 hours – occurred on 29 July 2013, when $T_{air} \geq 30^\circ\text{C}$ and heat stress appeared from 6 am to 5 pm, and UTCI_{high} reached 40.4 ($T_{air} = 36.3^\circ\text{C}$). The absolute heat load daily maximum in 2012–2022 occurred on August 8, 2013, when T_{air} was above the threshold of 30°C for nine successive hours and UTCI for 12 hours.

Discussion

Recently, the use of reanalysis data, offered in the ERA Land-5 sets, among others, has become increasingly popular, as it allows comprehensive analysis of thermal comfort studies for longer time series and any location, and furthermore with coverage of hourly data (Di Napoli *et al.* 2020). The use of satellite data sets – e.g., MODIS, MSG, SARA2, which offer data with even better spatial resolution – is another alternative (Wang *et al.* 2020; Danni *et al.* 2024). Therefore, in both cases, it should be borne in mind that the values of radiation fluxes, and ultimately the value of T_{mrt} estimated from them, may differ from the value estimated from a ground-based measurement (which may also be affected by measurement equipment used). That is valid especially in an area of complex topography (Gal, Kantor 2020) and also in areas with local climate significantly influenced by the share of greenery, e.g. adding vegetation decreases the mean radiant temperature by 10.5°C at noon (Jaafar *et al.* 2022). In addition, regardless of whether the data comes from numerical models or satellite soundings, such elements as biases due to clouds being too transparent for shortwave radiation (Hogan, Hirahara 2016), an underestimation of cloud occurrence, overestimation due to increased reflection or shortcomings in the simulated cloud microphysics may adjust the fluxes proportions (Carrer *et al.* 2019) and finally the value of T_{mrt} . Moreover, taking measurements and obtaining direct so-

lar radiation by simplification from shortwave total radiation as the beam reached the perpendicular plane in proportion to the solar zenith angle could be significantly overestimated at low solar altitude angles (Gal, Kantor 2020) and raise the value of T_{mrt} . In view of the above, the results of the occurrence of abundant heat load in the morning hours (Fig. 3) could be approached as possible but their number (total of 18 at 06 UTC per 2012–2022 period) with a degree of criticism. On the other hand, one cannot exclude the possibility that undisturbed by cloud cover, the solar input during these periods of the day was in fact significant and affected the occurrence of strong heat load conditions even before noon (Pecelj *et al.* 2020). An attempt to interfere with the value of CZA as to limit the potential overestimation of the flux on the perpendicular plane can lead to underestimation of UTCI during hours of the highest sun position, especially at the warm period of the year. That is why, in some cases, values of heat load by UTCI from ERA5 datasets for given locations and extreme occurrences seem to be lower than expected (Kruger, Napoli 2022). Evaluating the characteristics of UTCIs developed using different ways of estimating T_{mrt} and based on various input datasets (cloud cover or detailed radiative fluxes) can make the task difficult (Błażejczyk, Kuchcik 2021).

However, in addition to the problematic way of estimating T_{mrt} and UTCI, the choice of data analysed may raise questions about its representativeness. That refers in particular to body heat loads (expressed by UTCI) related to a user located in the street, while urban measurement stations are in great number located on roofs. To assess such a reference, it is necessary each time to take the surrounding conditions into account, i.e., the density of buildings, the conditions of use, and the characteristics of the ground. Results of such comparison (Griffith, McKee 2000) indicate that overcast skies lead to small rooftop-to-ground differences in both surface radiating temperature and air temperature. Observations show differences of $\sim 1^\circ\text{C}$ or less in radiating temperature and less than 1°C in air temperature. An exception was observed where a wall effect led to more than a 2°C difference in air temperatures between the roof and the ground. Differences on sunny summer days could be greater, in extreme conditions as high as 30°C in comparison to shaded and elevated unshaded points. That is related to solar energy absorbed by dark, unshaded surfaces compared to partially shaded urban street canyons. If the rooftop and pedestrian levels are

located in an area with similar artificial surface and albedo characteristics and well-ventilated, the differences in air and radiative temperature could be less than 1°C (Kim *et al.* 2022). In regard to the AGH station location, a similar effect can be expected.

For all the reasons mentioned above, although the research period partially coincides (August 2015 and June 2019), it is problematic to directly relate the results obtained to those presented by Twardosz (2023) – for both months, the average of UTCI values at 12 UTC was higher in the analysis presented here; $32.5 \pm 5.6^\circ\text{C}$ and $31.5 \pm 3.5^\circ\text{C}$ respectively. In the first case, it corresponded to the same UTCI category of moderate heat load and, in the second case, to the higher category of strong heat load. However, the percentage frequency of total occurrence of SH and VSH – 56% in August 2015 and 40% in June 2019, is similar to the results by Twardosz (2023). As summarised in Twardosz (2023), there was no severe heat stress during the evening hours in August 2015 and June 2019, selected as “unusually warm summer months”, while analysis using satellite data on radiation fluxes showed that it may have occurred four times in June 2019 at early morning (6 UTC). In general, based on the 2012–2022 analysis, during the warm part of the year (April–September), strong heat stress occurs in around 10% of cases. Krzyżewska *et al.* (2021) found out that Kraków has a higher proportion of such cases, as does Rzeszów, compared to other major Polish cities. However, short-term values may differ significantly depending on the location and the synoptic situation on a given day (Błażejczyk *et al.* 2022). This comparison mentioned above, like most of the ones found in publications, only applies to values of 12 UTC. There is no publication analysing the occurrence of SH in the daily cycle. Evanescent hourly analyses are only available for selected locations, months or limited to the heat wave period (Rozbicka, Rozbicki 2018) but also indicate episodic occurrence of morning UTCI values exceeding the severe heat stress threshold (Bryś, Ojrzyńska 2016). What is worth emphasising is that strong heat stress (SH) persists in Kraków not only around the thermal noon. However, it certainly occurs more often in the hours following solar noon (14–17 UTC), i.e., during thermal noon, than before noon (06–09 UTC). Early occurrence (06 UTC) of SH was reported in Serbia (Pecelj *et al.* 2020); however, there were more occurrences in July than in August, while in Kraków the proportion was the opposite. The shortwave radiation

input with good atmospheric transparency and relatively high sun position in the summer months can be crucial and sufficient to generate a high Tmrt value in the morning period. In addition, the slightly higher humidity (e.g., just exceeding 40%) contributes to the occurrence of high thermal load, although it drops significantly at mid-day. During the evening hours (18 UTC or later), even despite the increased contribution of upward longwave radiation, the persistence of elevated air temperature, and a renewed increase in humidity and/or sparse ventilation (occurrence of sensation of stuffiness) – the conditions assessed by UTCI in Kraków did not qualify for the severe heat stress category. Research on the temporal and spatial distribution of heat stress incidence in Sydney, which adopts an UTCI threshold of 26°C and is based on RayMan Tmrt calculations, demonstrates that it is subject to significant variation within the city area and is strongly modified by the complex of local meteorological and geographical conditions. And ultimately results in variation in the number of hours of exposure to heat stress – even by more than 100% (compared among city's locations for the highest and lowest frequency) with respect to exceeding the adopted threshold within a single metropolitan area (Sadeghi *et al.* 2021). Hence, it is advisable to make reference to location and to move away from using generalisations. Analogously, this applies to the approach to temporal data. On days defined as a “hot day” ($T_{\text{air}} \geq 30^\circ\text{C}$), the disparity in the duration of heat stress can be significant. Hence, guided only by the value of the extreme, some of the relevant information may be lost. Assuming, moreover, the generalisation that days with a higher hourly heat load will be proportionally fewer than those with a “shorter” occurrence of the significant heat load may not find coverage in reality. In Kraków in July, there are more days when the heat load persists for 3–5 hours in a 24-hour period than for just 1–2 hours. Those days with single hours of $\text{UTCI} \geq 32^\circ\text{C}$ in the analysed time were of a similar number as those when the heat load persisted for 6–8 hours in a 24-hour period. When the information to the public is delivered that a hot day is predicted to occur, but without additional information about the heat load severity relative to time, especially about prolonged exposure to heat, then such information is highly incomplete and may be misleading. As Kampmann and Bröde (2022) point out, a reliable assessment of the body's heat load should consider not only the momentary state but also an assessment over a longer period of exposure.

Also significant from the perspective of population shielding are the timing of the first episode with a significant heat load and the length of the season with the occurrence of such stressful conditions (Katavoutas, Founda 2019). These issues have been addressed in works where additional heat assessment metrics were proposed to be developed in weather warning systems (Sadeghi *et al.* 2021; Spangler *et al.* 2022). The results presented here indicate that prolonged daily abundant heat occurrence may occur with different UTCI_{high}. (taken as the highest hourly value of UTCI on a single day). Usually, the higher the UTCI_{high}., the more hours with the threshold of strong heat stress exceeded ($R^2=0.72$). Moreover, prolonged heat stress periods during the day may occur even on days when the threshold $\geq 30^\circ\text{C}$ is noted for one hour only (Fig. 4). And conditions with excessive heat burden, or unfavourable conditions conducive to overheating, can also occur at times before the air temperature exceeds the mentioned threshold. That can happen when the solar radiation is high enough, and the complex of other conditions is not conducive to the dissipation of heat from the surface of the skin. It can be then concluded that the negative impact of the heat load can be underestimated if the primary criterion is Tair only and other meteorological elements are excluded.

Conclusion

Given the availability of free hourly datasets derived from satellite systems or sets of reanalysis of numerical models, it would be advisable to extend bioclimatic analyses for Polish cities with hourly characteristics in opposition to the existing pattern for selected hours or daily average values. The introduction of impact assessments is necessary in more than half of the cases of negative and oppressive weather conditions resulting in heat stress that may be neglected in risk assessments and predictions using the basic thermal criterion only. The noon term value (UTCI₁₂) may not give a sufficient view of the expected maximum heat load on a given day. Moreover, the number of hours with a strong heat load varies significantly, even on days defined as “sweltering”. The above analysis demonstrates the urgent need to develop analyses and forecasts of the incidence of heat load based on comprehensive assessment indicators, such as UTCI. The development of such impact forecasts of heat load

on humans, undertaken by meteorological services in Poland, should additionally (except hourly values and the extremes) take into account the period of occurrence of excessive heat load conditions, similar to those proposed by Sadeghi *et al.* (2021) and Spangler *et al.* (2022), but including a threshold of $\text{UTCI} \geq 32$, as relevant to the potential negative effect in the Polish population as confirmed by epidemiological data. Heat load conditions during the warm season (April–September), occur not only on days classified as hot, which require proper shielding of the population and constant monitoring. It should also consider the prediction of the occurrence of a heatwave. However, the heatwave should be defined as a deviation from the norm. It represents a change in a relatively short time (Di Napoli *et al.* 2019) and is better justified from the point of view of the body's reaction than the exceedance of air temperature at the threshold. Forecasts for residents of urban areas should include parameterisation at a detailed spatial scale. Failure to include a detailed radiation balance and, thus, to run simulations without detailed topography and coverage will result in only approximate predictions and at a level analogous to a boundary layer urban heat island. The large variation in the complex of meteorological conditions can lead to significant differences in the category of heat load. Residents of Kraków should be educated about the potential negative impact of meteorological conditions on the body, the occurrence of which is not limited to hot days as well, which could vary spatially. Excessively stressful conditions for humans can appear as early as April and still occur in September. Considering the high seasonal and inter-annual variability of heat load conditions, it would be advisable to undertake actions aimed at using detailed heat load forecasts based on local urban morphology. In addition, educating the population about the effects of heat stress effects is needed.

References

- Błażejczyk K., Kuchcik M. 2021. UTCI applications in practice (methodological questions). *Geographia Polonica* 94(2): 153-165. 10.7163/GPol.0198
- Błażejczyk K., Twardosz J. 2023. Secular Changes (1826–2021) of Human Thermal Stress according to UCTI in Kraków (southern Poland). *International Journal of Climatology* 43(9): 4220-4230.

- Błażejczyk K., Epstein Y., Jendritzky G., Stäger H., Tinz B. 2012. Comparison of UTCI to selected thermal indices. *International Journal of Biometeorology* 56: 515-535.
- Błażejczyk K., Twardosz R., Wałach P., Czarnecka K., Błażejczyk A. 2022. Heat strain and mortality effects of prolonged central European heat wave—an example of June 2019 in Poland. *International Journal of Biometeorology* 66(1): 149-161.
- Bokwa A. 2019. Rozwój badań nad klimatem lokalnym Krakowa. *Acta Geographica Lodziensia* 108: 7-20.
- Bokwa A., Limanówka D. 2014. Effect of relief and land use on heat stress in Kraków, Poland. *Die Erde* 145(1–2): 34-48. DOI: 10.12854/erde-145-4
- Bokwa A., Hajto M.J., Walawender J.P., Szymanowski M. 2015. Influence of diversified relief on the urban heat island in the city of Kraków, Poland. *Theoretical and Applied Climatology* 122: 365-382.
- Bokwa A., Dobrovolný P., Gál T., Geletič J., Gulyás A., Hajto M.J., Holec J., Hollósi B., Kielar R., Lehnert M., Skarbit N., Šťastný P., Švec M., Unger J., Walawender J.P., Žuvela-aloise M. 2018. Urban climate in Central European cities and global climate change. *Acta Climatologica* 51–52: 7-35.
- Bokwa A., Geletič J., Lehnert M., Žuvela-Aloise M., Hollósi B., Gál T., Skarbit N., Dobrovolný P., Hajto M., Kielar R., Walawender J., Šťastný P., Holec J., Ostapowicz K., Burianová J., Garaj M. 2019. Heat load assessment in Central European cities using an urban climate model and observational monitoring data. *Energy and Buildings* 201: 53-69. DOI: 10.1016/j.enbuild.2019.07.023
- Brimicombe Ch., Quintino T., Smart S.D., Di Napoli C. 2022. Calculating the Cosine of the Solar Zenith Angle for Thermal Comfort Indices. *ECMWF Technical Memoranda* (online: <http://www.ecmwf.int/publications>).
- Bröde P., Fiala D., Błażejczyk K., Holmér I., Jendritzky G., Kampmann B., Tinz B., Havenith G. 2012. Deriving the operational procedure for the Universal Thermal Climate Index (UTCI). *International Journal of Biometeorology* 56(3): 481-94. DOI: 10.1007/s00484-011-0454-1
- Bryś K., Ojrzyńska H. 2016. Bodźcowość warunków biometeorologicznych we Wrocławiu. *Acta Geographica Lodziensia* 104: 193-200.
- Carrer D., Ceamanos X., Moparthy S., Vincent C., Freitas S., Trigo I.F. 2019. Satellite Retrieval of Downwelling Shortwave Surface Flux and Diffuse Fraction under All Sky Conditions in the Framework of the LSA SAF Program (Part 1: Methodology). *Remote Sensing* 11: 2532.
- Danni Z., Chang L., Jiansheng W., Hongliang W. 2024. A satellite-based approach for thermal comfort simulation: A case study in the GBA. *Urban Climate* 53: 101776.
- Di Napoli C., Pappenberger F., Cloke H.L. 2018. Assessing heat-related health risk in Europe via the universal thermal climate index (UTCI). *International Journal of Biometeorology* 62: 1155-1165.
- Di Napoli C., Pappenberger F., Cloke H.L. 2019. Verification of heat stress thresholds for a health-based heat-wave definition. *Journal of Applied Meteorology and Climatology* 58: 1177-1194.
- Di Napoli C., Hogan R.J., Pappenberger F. 2020. Mean radiant temperature from global-scale numerical weather prediction models. *International Journal of Biometeorology* 64: 1233-1245.
- Di Napoli C., Barnard C., Prudhomme C., Cloke H.L., Pappenberger F. 2020. Thermal comfort indices derived from ERA5 reanalysis. *Copernicus Climate Change Service (C3S) Climate Data Store (CDS)*. DOI: 10.24381/cds.553b7518
- Di Napoli C., Messeri A., Novak M., Rio J., Wiczorek J., Morabito M., Silva P., Crisci A., Pappenberger F. 2021. The Universal Thermal Climate Index as an Operational Forecasting Tool of Human Biometeorological Conditions in Europe. In: E.L. Krüger (ed) *Applications of the Universal Thermal Climate Index UTCI in Biometeorology*. *Biometeorology* 4. Springer, Cham.
- European Commission, Peseta IV – Projection of Economic impacts of climate change in Sectors of the European Union based on bottom-up, Online: [pesetaiv_summary_final_report.pdf](https://europa.eu/eu-attachments/press/pesetaiv_summary_final_report.pdf) (europa.eu)
- Gal C., Kantor N. 2020. Modeling mean radiant temperature in outdoor spaces. A comparative numerical simulation and validation study. *Urban Climate* 32: 100571.
- Geiger B., Carrer D., Franchistéguy L., Roujean J.L., Meurey C. 2008. Land surface albedo derived on a daily basis from Meteosat Second Generation observations. *IEEE Transactions on Geoscience and Remote Sensing* 46: 3841-3856. DOI:10.1109/TGRS.2008.2001798

- Griffith B.D., Mckee T.B. 2016. Rooftop and Ground Standard Temperatures: A Comparison of Physical Differences (online: <https://api.semanticscholar.org/CorpusID:127081326>)
- Hogan R.J., Hirahara S. 2016. Effect of solar zenith angle specification in models on mean shortwave fluxes and stratospheric temperatures. *Geophysical Research Letters* 43: 482-488.
- Hynčica M., Novák M., Procházková S. 2023. Trends and Climatology of UTCI in the Czech Republic. *Environmental Sciences Proceedings* 26(1): 31.
- Jaafar H., Lakkis I., Yeretzi A. 2022. Impact of boundary conditions in a microclimate model on mitigation strategies affecting temperature, relative humidity, and wind speed in a Mediterranean city. *Building and Environment* 210: 108712.
- Jendritzky G., de Dear R., Havenith G. 2012. UTCI – Why another thermal index? *International Journal of Biometeorology* 56: 421-428.
- Kampmann B., Bröde P. 2022. Do one-hour exposures provide a valid assessment of physiological heat strain? *Zeitschrift für Arbeitswissenschaft* 76: 105-117.
- Kántor N., Unger J. 2011. The most problematic variable in the course of human-biometeorological comfort assessment – the mean radiant temperature. *Central European Journal of Geosciences* 3: 90-100.
- Katavoutas G., Founda D. 2019. Intensification of thermal risk in Mediterranean climates: evidence from the comparison of rational and simple indices. *International Journal of Biometeorology* 63: 1251-1264.
- Kim B., Hwang S., Lee Y., Shin S., Kim K. Comparative analysis of environmental standards to install a rooftop temperature monitoring station. *Scientific Reports* 12(1): 22401.
- Kossowska-Cezak U., Twardosz R. 2014. Niezwykłe gorące miesiące i sezony letnie w Europie Środkowej i Wschodniej (1951–2010). Część II. Niezwykłe gorące sezony letnie. *Prace Geograficzne* 136.
- Krüger E.L., Di Napoli C. 2022. Feasibility of climate reanalysis data as a proxy for onsite weather measurements in outdoor thermal comfort surveys. *Theoretical and Applied Climatology* 149: 1645-1658.
- Krüger E.L., Minella F.O., Matzarakis A. 2014. Comparison of different methods of estimating the mean radiant temperature in outdoor thermal comfort studies. *International Journal of Biometeorology* 58: 1727-1737.
- Krüger E.L., Tamura C.A., Bröde P., Schweiker M., Wagner A. 2017. Short- and long-term acclimatization in outdoor spaces: exposure time, seasonal and heatwave adaptation effects. *Building and Environment* 116: 17-29.
- Kuchcik M. 2021. Mortality and thermal environment (UTCI) in Poland – long-term, multicity study. *International Journal of Biometeorology* 65: 1529-1541.
- Kuchcik M., Błażejczyk K., Halaś A. 2021. The stimuli of thermal environment defined according to UTCI in Poland. *Geographia Polonica* 94(2): 183-200. DOI:10.7163/GPol.0200
- Landsaf. 2023. Online: <https://landsaf.ipma.pt/en/> (last access: 30.12.2023).
- Liang S., Cheng C., Jia K., Jiang B., Liu Q., Xiao Z., Yao Y., Yuan W., Zhang X., Zhao X., Zhou J. 2021. The Global Land Surface Satellite (GLASS) products suite. *Bulletin of the American Meteorological Society* 102(1): E323-E337.
- Lindner-Cendrowska K., Baranowski J. 2023. Niepewność pomiarów średniej temperatury promieniowania za pomocą termometrów kulistych. *Przegląd Geograficzny* 95(3): 271-290.
- Martins J.P.A., Trigo I., Ghilain N., Jimenez C., Goettsche F.M., Ermida S., Olesen F., Gellens-Meulenberghs F., Arboleda A. 2019. An All-Weather Land Surface Temperature Product based on MSG/SEVIRI observations. *Remote Sensing* 11: 3044.
- Meade R.D., Notley S.R., Akerman A.P., McGarr G.W., Richards B.J., McCourt E.R., King K.E., McCormick J.J., Boulay P., Sigal R.J., Kenny G.P. 2023. Physiological responses to 9 hours of heat exposure in young and older adults. Part I: Body temperature and hemodynamic regulation. *Journal of Applied Physiology* 135(3): 673-687.
- Ministry of the Environment, Urban Adaptation Plans for in cities with over 100 thousand inhabitants (online: <http://44mpa.pl/miejskie-plany-adaptacji/>; access 22.12.2023)
- Miranda N.D., Lizana J., Sparrow S.N., Zachau-Walker M., Watson P.A.G., Wallom D.C.H., Khosla R., McCulloch M. 2023. Change in cooling degree days with global mean temperature rise increasing from 1.5 °C to 2.0 °C. *Nature Sustainability* 6: 1326-1330.

- Niedźwiedz T., Obrebska-Starkłowa B., Limanówka D., Mroczka A., Ustrnul Z. 1996. Zmienność bioklimatu Krakowa. *Folia Geographica. Series Geographica-Physica* 26–27: 89-105.
- Okoniewska M. 2021. Daily and seasonal variabilities of thermal stress (based on the UTCI) in air masses typical for Central Europe: an example from Warsaw. *International Journal of Biometeorology* 65: 1543-1552.
- Pecelj M.M., Lukić M.Z., Filipović D.J., Protić B.M., Bogdanović U.M. 2020. Analysis of the Universal Thermal Climate Index during heat waves in Serbia. *Natural Hazards and Earth System Sciences* 20: 2021-2036.
- Peres L.F., DaCamara C.C. 2005. Emissivity maps to retrieve land-surface temperature from MSG/SEVIRI. *IEEE Transactions on Geoscience and Remote Sensing* 43(8): 1834-1844.
- ProClias Project. 2023. Online: <https://proclias.eu/working-groups/wg3/tg3-11> (last access: 22.12.2023).
- Romaszko J., Dragańska E., Jalali R., Cymes I., Glińska-Lewczuk K. 2022. Universal Climate Thermal Index as a prognostic tool in medical science in the context of climate change: a systematic review. *Science of The Total Environment* 828: 154492.
- Rozbicka K., Rozbicki T. 2018. Variability of UTCI index in South Warsaw depending on atmospheric circulation. *Theoretical and Applied Climatology* 133: 511-520.
- Sadeghi M., de Dear R., Morgan G., Santamouris M., Jalaludin B. 2021. Development of a heat stress exposure metric – impact of intensity and duration of exposure to heat on physiological thermal regulation. *Building and Environment* 200: 107947.
- Spangler K.R., Liang S., Wellenius G.A. 2022. Wet-Bulb Globe Temperature, Universal Thermal Climate Index, and Other Heat Metrics for US Counties, 2000–2020. *Scientific Data* 9: 326.
- Tomczyk A.M., Matzarakis A. 2023. Characteristic of bioclimatic conditions in Poland based on Physiologically Equivalent Temperature. *International Journal of Biometeorology* 67: 1991-2009.
- Trigo I.F., Peres L.F., DaCamara C.C., Freitas S.C. 2008. Thermal Land Surface Emissivity Retrieved From SEVIRI/Meteosat, *IEEE Transactions on Geoscience and Remote Sensing* 46: 307-315.
- Trigo I.F., Barroso C., Viterbo P., Freitas S.C., Monteiro I.T. 2010. Estimation of Downward Longwave Radiation at the Surface combining Remotely Sensed Data and NWP Data. *Journal of Geophysical Research* 115: D24118.
- Twardosz R. 2023. Obciążenia cieplne człowieka podczas niezwykle ciepłych miesięcy letnich w Krakowie. *Przegląd Geograficzny* 95(3): 255-270.
- Urban A., Huber V., Henry S., Plaza N.P., Dasgupta S. 2023. Do heat prevention measures reduce the risk of heat-related mortality in Europe? EMS Annual Meeting 2023, Bratislava, Slovakia, 4–8 September 2023, EMS2023-133. <https://doi.org/10.5194/ems2023-133>, 2023.
- Ville de Paris. 2023. Mission information et d'évaluation du conseil de Paris, Le rapport: Paris a 50°C https://cdn.paris.fr/paris/2023/04/21/paris_a_50_c-le_rapport-Jc4H.pdf (last access 22.12.2023).
- Wang C., Zhan W., Liu Z., Li J., Li L., Fu P., Huang F., Lai J., Chen J., Hong F., Jiang S. 2020. Satellite-based mapping of the Universal Thermal Climate Index over the Yangtze River Delta urban agglomeration. *Journal of Cleaner Production* 277: 123830.